Ordering-induced direct-to-indirect band gap transition in multication semiconductor compounds

Ji-Sang Park, Ji-Hui Yang, Ana Kanevce, Sukgeun Choi, Ingrid L. Repins, and Su-Huai Wei

Phys. Rev. B **91**, 075204 — Published 17 February 2015

DOI: 10.1103/PhysRevB.91.075204

Ordering-induced direct to indirect band gap transition in multi-cation semiconductor compounds

Ji-Sang Park, Ji-Hui Yang, Ana Kanevce, Sukgeun Choi, Ingrid L. Repins, and Su-Huai Wei

National Renewable Energy Laboratory, Golden, CO, USA 80401

ABSTRACT

Using first-principles calculations and symmetry analysis, we show that as cation atoms in a zincblende-based semiconductor are replaced through atomic mutation (e.g., evolve from ZnSe to $CuGaSe_2$ to $Cu_2ZnGeSe_4$), the band gaps of the semiconductors will become more and more indirect because of the band splitting at the zone boundary, and in some cases will even form the segregating states. For example, although ZnSe is a direct band gap semiconductor, quaternary compounds $Cu_2ZnGeSe_4$ and $Cu_2ZnSnSe_4$ can be indirect band gap semiconductors if they form the primitive mixed CuAu ordered structures. We also find that the stability and the electronic structure of the quaternary polytypes with different atomic ordering are almost negative-linearly correlated. We suggest that these intrinsic properties of the multi-cation semiconductors can have a large influence on the design and device performance of these materials.

I. Introduction

Quaternary semiconductor compounds such as Cu_2ZnSnS_4 (CZTS), $Cu_2ZnSnSe_4$, (CZTSe), and $Cu_2ZnSn(Se_{1-x}Se_x)_4$ (CZTSSe) have emerged as new and important thin-film solar cell absorber materials in the last few years. This is because they contain relatively earth abundant elements, are easy to grow, and have suitable direct band gap energies in the range of 1 to 1.5 eV at their ground state,[1-5] which are optimal for single junction solar cell applications.[3,6] However, despite the recent extensive study and rapid progress in development of this new solar cell technology, its power conversion efficiency is still lower than the more mature technologies, such as binary CdTe or ternary $Cu(In_{1-x}Ga_x)Se_2$ (CIGSe) based solar cells. One of the main issues is that the open circuit voltage (V_{OC}) of the CZTSSe-based solar cell is apparently lower than CdTe- and CIGSe-based solar cells, despite them having similar band gaps.[7] One of the possible reasons could be that CZTSSe as quaternary (or pseudoquaternary) compounds can have many different cation atomic configurations and associated band structures coexisting in the sample, which may lead to band edge energy fluctuation and band tailing,[8] thus hindering the enlargement of the V_{OC}.[9] However, unlike their binary and ternary counterparts, the band structure of the quaternary adamanites has not yet been carefully studied in the past, especially the manner in which ordering or disordering in the cation sublattice affects the band structures. Therefore, to understand the general chemical trend and further improve the CZTSSe solar cell efficiency, a comprehensive study of the stability and the electronic structures of CZTSSe polytypes is needed.

The atomic structure of the quaternary compounds such as CZTSe can be obtained by applying sequential cation mutation,[10] starting from II-VI zinc-blende (ZB) compounds as shown in Fig. 1. For example, the I-III-VI_2 compound $CuGaSe_2$ (CGSe), which has a chalcopyrite (CH)

ground state structure, can be obtained from ZnSe by replacing the two group-II Zn atoms with a group-I Cu atom and a group-III Ga atom. Similarly, $Cu_2ZnGeSe_4$ (CZGSe), which has a kesterite (KS) ground-state structure, can be obtained from CGSe by replacing every two group-III Ga atoms by a group-II Zn atom and a group-IV Ge atom. As the cation mutation is applied, the symmetry and the electronic structure of the materials are modified. Therefore, a cation mutation can be an effective way to enlarge the selectivity of material properties for specific device applications.[10] On the other hand, when the number of cations increases in the compound, more different ordered or disordered cation atomic configurations are possible in the sample. Also, the electronic band structures, such as the band gap and the directness of the band gap (i.e., the difference between the minimum direct and indirect band gap), can depend sensitively on the atomic configuration.[10,11]

Using first-principles total energy and band structure calculations based on the hybrid functional, we find that cation ordering in CZTS and CZTSe can reduce the direct band gap by several hundreds of meV compared to the ground state KS structure, despite only a few meV per atom difference in the formation energy among different polytypes that satisfy the octet rules. Moreover, contradictory to the common belief that CZTSSe is a direct band gap material, we find that these quaternary compounds in the primitive mixed CuAu (PMCA) structure[10] have indirect band gap with a valence band maximum (VBM) at the Γ point and conduction band minimum (CBM) at the A points in the PMCA Brillouin zone (BZ). The reason for the development of the indirect band gap in the quaternary compounds is mainly ascribed to the emergence of the symmetry-induced segregating states.[11] Because of the small energy difference among the polytypes, which is almost linearly and negatively correlated with the band gap, different cation-ordered phases can coexist in these compounds.[10,12-15] This large variation of

band structure as a function of atomic configuration, therefore, could be one of the reasons for the observed V_{OC} deficit in this system, because the spatial fluctuation of the band edge states can reduce the effective band gap of the solar absorber.[7,16-18] Therefore, the intrinsic properties of the multi-cation semiconductors can have a large influence on the design and device performance of these materials.

II. Methods of the Calculations

First-principles total energy and band structure calculations are performed within the density functional theory. We use the Vienna ab-initio Simulation Package (VASP)[19] and projector-augmented wave (PAW) pseudo-potentials to describe electron-core interactions.[20] The hybrid functional suggested by Heyd, Scuseria, and Ernzerhof (HSE) is used to describe the exchange correlation interactions,[21] which reproduces the experimentally determined band gap. The Sn *d* states are treated explicitly as valence states. The cutoff energy for the plane-wave basis is 295 eV. For BZ integration, we used *k* point meshes that are equivalent to the 4 × 4 × 4 Monkhorst-Pack meshes for an eight-atom cubic unit cell.[11] The atomic structures are optimized until the residual forces are less than 0.03 eV/Å.

III. Results and Discussions

To analyze how the states are evolved when the cation mutation is applied, we first calculate and compare the electronic band structure of binary ZnSe, ternary CGSe, and quaternary CZGSe, whose atomic structures are shown in Fig. 1. Because the mutated cations are in the same row of the Periodic Table, these compounds have similar lattice constants. So to check and isolate the chemical effects of the cation mutation, we initially fix the lattice constants and the internal coordinates of the materials to those of bulk ZnSe. We calculate the electronic band structure of

CZGSe in body-centered-tetragonal KS (space group I-4) and stannite (ST) (space group I-42m) structures and simple tetragonal PMCA (space group p-42m) structure that are depicted in Fig. 1 (d-f). The primitive cells of these superstructures contain four primitive ZB cells; therefore, the *k* points in the BZ of the primitive supercell are folded from four *k* points in the ZB BZ, as shown in Table 1. For example, two Σ and two L points in the ZB BZ are folded to the N point in the KS BZ and the four L points in ZB BZ are folded to the A point in the PMCA BZ.

The calculated band structures are plotted in Fig. 2. The first column shows the electronic band structures of (a) ZnSe, (d) CGSe, and (g) CZGSe in the primitive cell of the PMCA structure with c/a=1. The second column shows the band structures in the primitive cell of the ST structure, and the third column shows the band structures in the primitive cell of the KS structure. For these compounds, the top of the valence bands are composed mainly of Se *p* and cation *d* states and the bottom of the conduction bands are mainly cation *s* and anion *s* states. From Fig. 2, we can see that as the cation mutation is applied, it has large effects on the band structure of these compounds because of the reduced symmetry. For example, for ZnSe, the lowest four conduction band (CB) states at the A point of the PMCA BZ are folded from the 4L points in the ZB BZ (Table I); therefore, the CBM at the A point is a four-fold degenerate [Fig. 2(a)]. When 2Zn is mutated to Cu+Ga forming CGSe, these four levels split. The lowest doubly degenerate CB states at A become segregating states with *s* orbital charge only on Ga sites (green), whereas the second lowest doubly degenerate CB states have *s* orbital charge only on Cu sites (red; there are always charges on anion sites, so they are not explicitly discussed here). Because of the level splitting and charge segregation,[11] the CBM energy differences between the Γ and A point decreases, and thus the band gap character become less direct. When we further replace 2Ga atoms by Zn+Ge, forming CZGSe, the doubly degenerate lowest energy level at the

A point splits again. The lowest energy conduction band at A point is pushed down by s orbital only on the Ge site (green) because Ge has the lowest *s* orbital energy among the three cations. As expected, the second and the third (doubly degenerate) lowest conduction band states at A have *s* orbital only on Zn (green) and Cu (red) sites, respectively. On the other hand, the CBM at the Γ point has charge more localized at the Ge site, but it has non-zero *s* wavefunction at both the Cu and Zn sites (less bluish). Therefore, the energy lowering of the CBM at Γ due to the atomic mutation is smaller than that at the A point. Because of this large level splitting and wavefunction segregation, for the PMCA structure, the CBM at the A point now has lower energy than that at the Γ point. Therefore, the atomic mutation turns the direct band gap semiconductor ZnSe into an indirect band gap PMCA-CZGSe. Similar trends are also found for the ST and KS structures. We find that because of symmetry-induced level splitting and wavefunction localization at the BZ boundary (N point), CZGSe in KS and ST ordered structures are almost indirect band gap semiconductors.

As discussed above, PMCA CZGSe has an indirect band gap. When Ge is replaced by Sn, we find that if the anion displacement parameter is set to 1/4, i.e., at the ideal ZB sites, then the conduction band edge energy at the A point is slightly higher than that at the Γ point by about 0.1 eV. This is because the atomic 5*s* orbital of Sn is not as deep as the 4*s* orbital of Ge, so the splitting at the A point is not as large. But, the situation changes when the atomic position is fully relaxed. In this case, the Sn-Se bond length increases significantly and the Cu-Se and Zn-Se bond lengths are reduced, causing the CBM at the A point to be about 0.1 eV lower than that at Γ. This is because the Γ point antibonding CBM state also has Cu and Zn components, compared to the segregating CBM state at the A point that has *s* orbital only on the Sn site. Therefore, when the bond lengths relax, the energy drop at the A point is larger than that at the Γ point,

which makes the system indirect band gap. For PMCA-CZTS, however, we find that it has a direct band gap although the conduction band edge at the A point in the tetragonal cell is only about 5 meV higher than that at the Γ point. This is also because the CBM at the A point has a larger deformation potential than that at Γ. So when the lattice constant decreases because of the change from Se to S, the upward shift of the antibonding CBM states at A is larger than that at Γ. We want to point out that the indirect band gap of PMCA CZTSe is not because of mixing of the exact exchange. Our PBE+U_d (U_d = 6 eV) calculation also find that the band gap is indirect; the conduction band edge (CBE) at the A point is 40 meV lower than the CBE at the Γ point.

In the previous analysis, we discussed the band structures of three small unit cell CZGSe polytypes that satisfy the octet rule. It is expected that structures that do not obey the octet rule will have higher energy, and therefore are less likely to form. As we will show subsequently, the material properties of the quaternary polytypes that satisfy the octet rule can be obtained as a linear combination of material properties of the three fundamental structures. In the following discussion, without losing generality, we will use CZTS and CZTSe as examples because they are more popularly used for solar cell application than CZGSe. We will first develop a scheme to classify these quaternary compounds. Figure 1 (d-f) shows the atomic structures of PMCA, ST, and KS. In principle, there are three basic operations, such as the interchange of Cu and Zn (Cu_{Zn}+Zn_{Cu}), Cu and Sn (Cu_{Sn}+Sn_{Cu}), and Zn and Sn (Zn_{Sn}+Sn_{Zn}). We find that there are only three basic operations associated with these three atomic exchanges to generate all the structures that satisfy the octet rule. Two of them are shifting the entire (001) planes by (a/2, a/2, 0) relative to the same plane in the KS structure (Fig. 1). The first operation is shifting a (001) plane containing Cu and Zn atoms, and the second operation is shifting the other (001) plane containing Cu and Sn atoms. By using these operations, the atomic structure of PMCA, for

example, can be obtained from the KS structure by shifting two adjoining (001) planes together for every four layers. (Note that in the achieved PMCA structure, the *x* and *z* direction is switched compared to that shown in Fig. 1.) The third operation is shifting the entire Zn and Sn (001) planes by (a/2, a/2, 0) relative to the same plane in the ST structure (Fig. 1). In this case, the PMCA structure can be obtained from the ST structure by shifting alternatively one of the two adjoining Zn and Sn (110) planes. Because we can randomly and individually apply the three operations, an infinite number of polytypes that satisfy the octet rule can be generated.

To understand the chemical trends of the stability and band gap of the polytypes, we have developed an Ising model[22] to describe the quaternary polytypes. Because we consider three operations, three different pair interactions are used to describe the formation energy E_f (per 4 atoms): (1) the pair interaction between the (001) layers containing Cu and Zn is denoted by J_{I+II}, ; (2) the pair interaction among the (001) layers containing Cu and Sn is given by J_{I+IV}; (3) the interaction between the (001) layers containing only Zn and Sn is indicated by J_{II+IV}. The first two parameters are used to describe the polytypes changing between KS and PMCA while the third parameter is needed for the polytypes changing between ST and PMCA. The Ising model to describe E_f for the polytypes σ between KS and PMCA is given by

$$E_f(\sigma) = J_{0,\mathrm{KS-PMCA}} + \Pi_{\mathrm{I+II}}(\sigma)J_{\mathrm{I+II}} + \Pi_{\mathrm{I+IV}}(\sigma)J_{\mathrm{I+IV}}, \quad (1)$$

On the other hand, for the polytypes between ST and PMCA,

$$E_f(\sigma) = J_{0,\mathrm{PMCA-ST}} + \Pi_{\mathrm{II+IV}}(\sigma)J_{\mathrm{II+IV}}. \quad (2)$$

Here, the layer correlation function Π for configuration σ is given by

$$\Pi(\sigma) = \frac{1}{2N}\sum_{i=1}^{N}[1 + S_i(\sigma)S_{i+2}(\sigma)], \quad (3)$$

where *N* is the layer period of the polytype. The layer spin variable S_i is 1 or -1 if the layer is unshifted or shifted, respectively, with respect to the planes of the reference structure (KS for Eq.

(1) and ST for Eq. (2)). It is clear that with this definition, the layer correlation function for the reference KS and ST structures are all equal to 1 and for PMCA structure it is -1. Therefore, with these interaction parameters, the material properties of all the polytypes satisfying the octet rule are bound between KS and PMCA, and between ST and PMCA.

We have calculated the relative formation energies for CZTS and CZTSe (with respect to the KS structure) and the band gaps for some of the polytypes. For these calculations, the lattice constants and the internal coordinates are fully optimized. As shown in Fig. 3, the formation energy and the band gap of the polytypes are indeed bounded by those of KS and PMCA structures, indicating that our assumption of short-range layer-to-layer interaction is reasonable. The KS structure has the largest band gap and lowest formation energy whereas the PMCA structure has the smallest band gap and highest formation energy, which suggests that the band gap is negatively correlated with the formation energy of the polytypes. This result is consistent with previous calculations showing that the KS phase is more stable than the PMCA and ST phases, and the band gap of the KS phase is larger than the others.[10,12,13]

We can fit the calculated formation energies of a few small supercell structures into the Ising model to obtain the interaction parameters, and then obtain the formation energies for all the other structures using the fitted parameters. The fitted interaction parameters are shown in Table 2. The table clearly shows that the stability of the polytypes is mainly controlled by the Cu-Sn layer ordering. The Zn-Sn layer ordering makes a relatively smaller effect because it influences only the ordering with ST and PMCA as the two end point constituents, and they are both derived from the CuAu (CA) structure of the ternary compounds.[10] The effect of Cu-Zn ordering is the smallest, consistent with the fact that Cu and Zn are same row neighbors in the Periodic Table. So they cause the least perturbation to the original KS structure. However, the formation

energy difference between all the polytypes is rather small, suggesting that many of the different polytypes may coexist in the sample. Considering that PMCA CZTS and CZTSe have band gaps about 0.3 eV lower than their KS counterparts and CZTSe even has an indirect band gap, it is very likely that the coexistence of the different phases will effectively reduce the band gap and thus V_{oc}.

Experiment studies show that the band gap of CZTSe is around 1 eV,[4,18] however, it generally decreases with increasing of the annealing temperature, and the deviation of the band gap is as large as 0.12 eV.[18] Our calculation shows that lower band gap polytypes have higher formation energy, which are more likely to form as temperature increases, resulting in the reduced band gap. As the temperature increases, the atomic correlation functions in the Ising model become close to 0, i.e., making the system more random. The relative formation energy of this random polytype is about half of the PMCA polytype, thus following the negative-linear-correlation between formation energy and band gap, the band gap of the random polytype is reduced by around 0.15 eV with respect to the band gap of KS CZTSe, consistent with experiment results.

To put this into perspective, we compare CZTSe with CISe, which have similar band gaps, in terms of stability and band structure variation of the polytypes. Using the HSE hybrid functional calculation, we find that the formation energy of CA-CISe is higher by about 3 meV per atom, and the band gap of the CA phase is 0.14 eV smaller than the CH phase. Because the band gap reduction is low, compared to CZTSe, CIGSe has more spatially uniform band gap and higher V_{OC}, which is consistent with experimental observations showing that a CZTSe sample is more disordered at the cation site and has lower power conversion efficiency.[8]

IV. Conclusions

In summary, we show that CZTSe with specific atomic ordering can have an indirect band gap, and this is because the existence of the multi-cation lowers the crystal symmetry and leads to emergence of the segregating states at the BZ boundary, which significantly lowers its band edge energy. All the quaternary CZTSe polytypes satisfying the octet rule are classified, and their stability and the electronic structure are investigated using an Ising model and found to be linearly and negatively correlated. Fluctuation of the band edges in the quaternary CZTSe compound is much stronger compared to the ternary CIGS, which is considered to be one of the reasons that the quaternary compounds have lower expected efficiency.

Acknowledgements

The Work at NREL was supported by the U.S. Department of Energy, EERE, under Contract No. DE-AC36-08GO28308.

REFERENCES

1. T. K. Todorov, J. Tang, S. Bag, O. Gunawan, T. Gokman, Y. Zhu, and D. B. Mitzi, Adv. Energy Mater. **3**, 34 (2013).

2. S. Chen, A. Walsh, X.-G. Gong, and S.-H. Wei, Adv. Mater. **25**, 1522 (2013**)**.

3. A. Polizzotti, I. L. Repins, R. Noufi, S.-H. Wei, D. B. Mitzi, Energy Environ. Sci. **6**, 3171 (2013).

4. L. Gu□tay, A. Redinger , R. Djemour , and S. Siebentritt, Appl. Phys. Lett. **100**, 102113 (2012).

5. Q. Shu, J.-H. Yang, S. Chen, B. Huang, H. Xiang, X.-G. Gong, and S.-H. Wei, Phys. Rev. B **87**, 115208 (2013).

6. W. Shockley and H. J. Queisser, J. Appl. Phys. **32**, 510 (1961).

7. W. Wang, M. T. Winkler, O. Gunawan, T. Gokmen, T. K. Todorov, Y. Zhu, and D. B. Mitzi, Adv. Energy Mat. **4**, 1301465 (2014).

8. T. Gokmen, O. Gunawan, T. K. Todorov, and D. B. Mitzi, Appl. Phys. Lett. **103**, 103506 (2013).

9. U. Rau, P. O. Grabitz, and J. H. Werner, Appl. Phys. Lett. 85, 6010 (2004).

10. S. Chen, X. G. Gong, A. Walsh, and S.-H. Wei, Phys. Rev. B **79**, 165211 (2009).

11. S.-H. Wei and A. Zunger, Phys. Rev. B **39**, 3279 (1989).

12. C. Persson, J. Appl. Phys. **107**, 053710 (2010).

13. Y. Zhang, X. Sun, P. Zhang, X. Yuan, F. Huang, and W. Zhang, J. Appl. Phys. **111**, 063709 (2012).

14. A. Khare, B. Himmetoglu, M. Johnson, D. J. Norris, M. Cococcioni, and E. S. Aydil, J. Appl. Phys. **111**, 083707 (2012).

15. R. Djemour, A. Redinger, M. Mousel, L. Gütay, and S. Siebentritt, J. Appl. Phys. **116**, 073509 (2014).

16. S. Schorr, Sol. Energ. Mat. Sol. C. **95**, 1482 (2011).

17. J. J. S. Scragg, L. Choubrac, A. Lafond, T. Ericson, and C. Platzer-Björkman, Appl. Phys. Lett. **104**, 041911 (2014).

18. G. Rey, A. Redinger, J. Sendler, T. P. Weiss, M. Thevenin, M. Guennou, B. El Adib, and S. Siebentritt, Appl. Phys. Lett. **105**, 112106 (2014).

19. G. Kresse and J. Furthmüller, Phys. Rev. B **54**, 11169 (1996).

20. P. E. Blöchl, Phys. Rev. B **50**, 17953 (1994).

21. J. Heyd, G. E. Scuseria, and M. Ernzerhof, J. Chem. Phys. **118**, 8207 (2003).

22. S.-H. Wei, S. B. Zhang, and A. Zunger, Phys. Rev. B **59**, R2478 (1999).

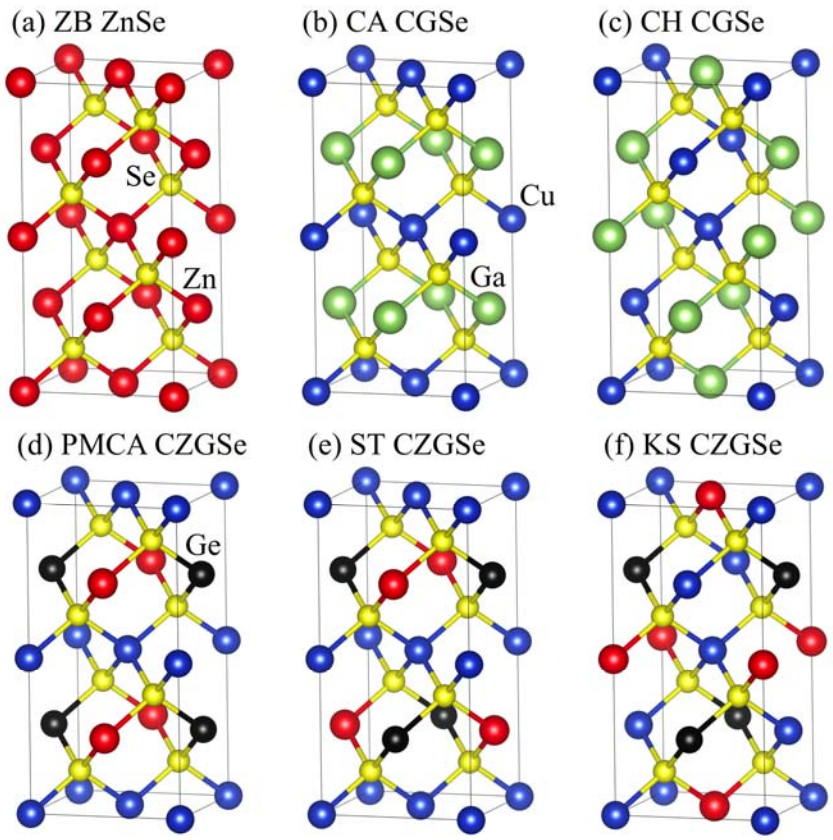

Figure 1. The atomic structures of Zinc-blende (ZB), CuAu (CA), Chalcopyrite (CH), primitive mixed CuAu (PMCA), Stannite (ST), and Kesterite (KS). Red, yellow, blue, green, and black spheres denote Zn, Se, Cu, Ga, and Ge atoms, respectively.

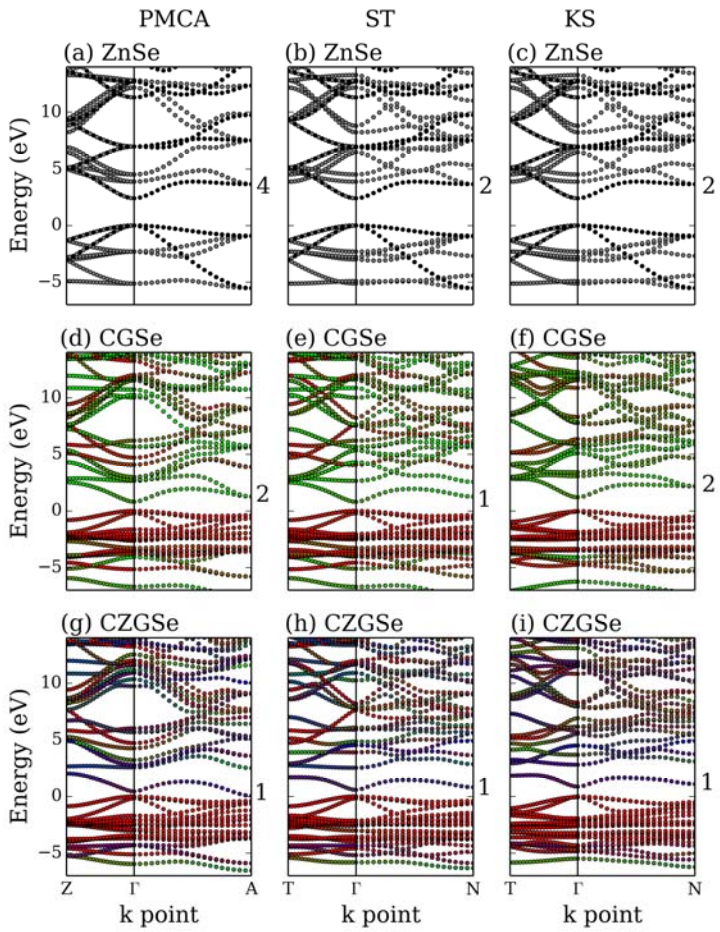

Figure 2. The electronic band structure of (a-c) ZnSe, (d-f) CGSe, and (g-i) CZGSe in the primitive cell of (a, d, g) PMCA, (b, e, h) ST, and (c, f, i) KS. Both KS and ST are in a body-centered tetragonal structure whereas PMCA is in a simple tetragonal structure. In the first row, black dots are the original ZB states and the grey dots are the ones folded from other k points in the ZB BZ. In the second row, green and red colors represent the percentage of Ga and Cu character among cations, respectively. In (d) and (e), the band of CuAu CGSe is shown. For comparison, in (f), the band of CH CGSe is shown. In the third row, red, green, and blue colors represent the percentage of Cu, Zn, and Ge character among cations, respectively. The numbers in the vicinity of the conduction band edge indicate degeneracy of the states.

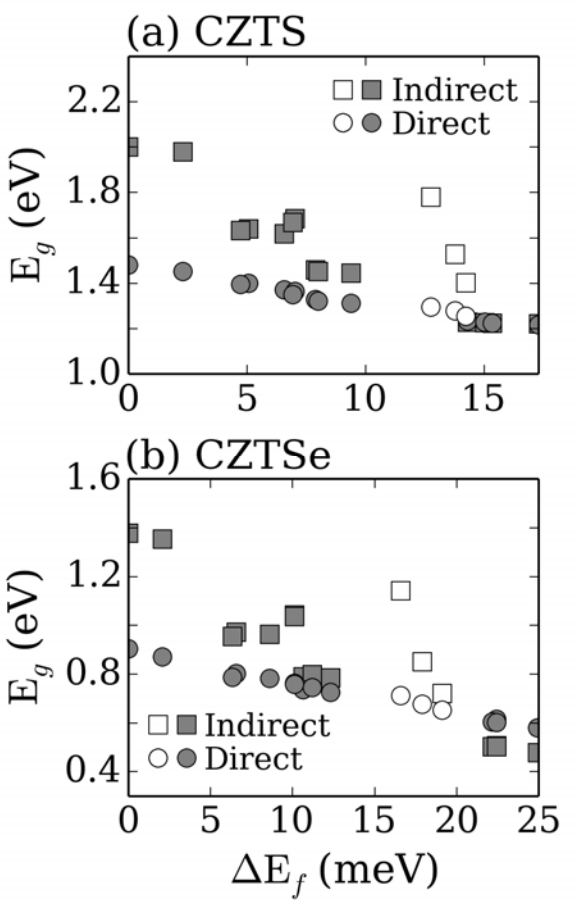

Figure 3. The electronic band gap as a function of the relative formation energy per 4 atoms. The formation energies of KS CZTS or CZTSe is set to 0 eV. Circles and boxes represent the direct and indirect band gap, respectively; gray circles and boxes represent the polytypes between KS and PMCA, and white circles and boxes represent the polytypes between ST and PMCA.

Table 1. Folding relationship between the special *k* points of the zinc-blende BZ and the superstructure BZ.

Superstructure	k points in superstructure	k points in ZB
Body centered tetragonal	T	2 X, 2 Δ
	Γ	Γ, 2 W, X
	N	2 Σ, 2 L
Tetragonal	Z	2 W, 2 Δ
	Γ	Γ, 3 X
	A	4 L

Table 2. The fitted interaction parameters for the relative formation energy (ΔE_f in meV per 4 atoms) with respect to that of KS. The maximum fitting error (δE) between the first-principles result and the fitted lines are also shown.

	$J_{0,KS\text{-}PMCA}$ (meV)	J_{I+II} (meV)	J_{I+IV} (meV)	$J_{0,PMCA\text{-}ST}$ (meV)	J_{II+IV} (meV)	δE (meV)
CZTS	8	-1	-7	15	-2	2
CZTSe	12	-1	-11	21	-4	2